Multimodal Solutions to Augmented Moore-Greitzer Model and Rotating Stall

Amit Kumar* , N. Ananthkrishnan† , and B. Roy‡
Indian Institute of Technology - Bombay, Mumbai 400076, India

The Moore-Greitzer model predicts rotating stall at the peak of the compressor characteristic. The model is augmented to enable it to predict onset of rotating stall to the right of the peak of the compressor characteristic. This is done through introduction of a variable r which is a measure of the flow incidence angle at the reference mean of the compressor. Bifurcation analysis of augmented Moore-Greitzer model is carried out to find the point of onset of rotating stall.

Nomenclature

A_k	Amplitude of k^{th} harmonic of disturbance potential
B	Greitzer parameter proportional to compressor speed at half radius
C_{w1}	Circumferential velocity at rotor inlet
C_{w1R}	Circumferential velocity at radius R
J	Square of amplitude of fundamental harmonic
l_c	Total aerodynamic length of compressor and ducts, in wheel radii
q	Parameter in modified Moore-Greitzer model
m	Compressor duct parameter
r	Variable introduced to modify Moore-Greitzer model
R	Radius of the compressor
R_m	Geometric mean radius of compressor
R_P	Reference mean radius of compresor
Y	Non-dimensionalized disturbance potential at compressor entrance
α_1	= Phase lock angle between first and second mode $(2\Theta_1 - \Theta_2)$
β	Scaled B
β_1'	Rotor blade inlet angle
Φ	Non-dimensionalized axial flow coefficient
Φ_m	Φ at geometric mean of augmented Moore-Greitzer model
Φ_p	Φ at reference mean of augmented Moore-Greitzer model
Φ_R	Φ at radius R
$\tilde{\phi}'$	Disturbance velocity potential
γ	Throttle parameter
Θ_k	Phase of k^{th} harmonic of disturbance potential
θ	Angular coordinate
Ψ	Non-dimensionalized total-to-static pressure rise coefficient

I. Introduction

Axial compressor instabilities, namely, stall and surge, have been a constant source of problems for aircraft engine designers. There have been a number of models proposed for the prediction as well as for

*Dual Degree Student, Department of Aerospace Engineering, amit@aero.iitb.ac.in.
†Associate Professor, Department of Aerospace Engineeringi akn@aero.iitb.ac.in. Senior Member AIAA.
‡Professor, Department of Aerospace Engineering, aeroyia@aero.iitb.ac.in. Senior Member AIAA.

understanding the mechanism of compressor instability.[1] One of the universally accepted models is the Moore-Greitzer model.[2] The basic compression system of the Moore-Greitzer model is shown in Fig. 1. It consists of a compressor operating in a duct and discharging to a downstream plenum. The plenum dimensions are large compared to those of the compressor and its ducts, so that the velocities and fluid accelerations in the plenum can be considered negligible. Hence, the pressure in the plenum can be considered to be spatially uniform although possibly varying in time. The flow through the system is controlled by a throttle at the plenum exit.

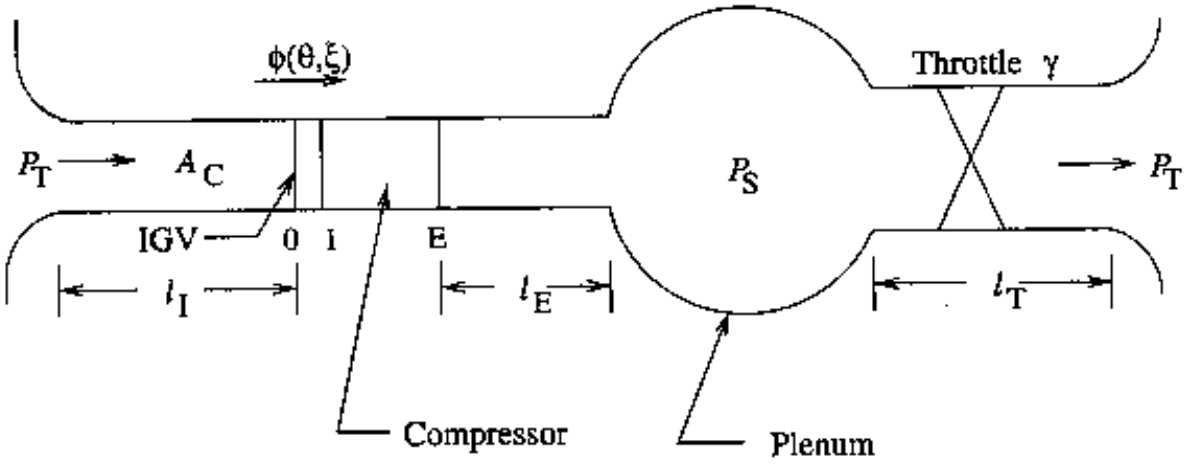

Figure 1. Schematic of axial compression system

The model finally gives three differential equations in three non-dimensional variables: total-to-static pressure rise coefficient (Ψ), axial flow coefficient (Φ), and disturbance potential at compressor face (Y). These equations can be simplified using Galerkin procedure and by assuming cubic axisymmetric characteristic for the compressor. This will be shown in the subsequent sections.

In the present work, we will be concentrating on rotating stall and its inception. Rotating stall is a local instability phenomenon in which one or more regions of stalled flow called 'stall cells' rotate around the circumference of the compressor. Day,[3] and Camp and Day,[4] have shown that stall inception can occur by two types of disturbances. The first one is due to the longer length-scale disturbance known as a 'modal oscillation' while the other is due to the shorter length-scale disturbance known as a 'spike'. The Moore-Greitzer model is valid only for modal disturbances. It predicts that the stall inception occurs at the peak or to the left of the peak of the compressor characteristic curve. But, from practical experience, it is known that the compressor can stall to the right of the peak as well. Camp and Day has attributed this to the spiky disturbance.

Camp and Day[4] have shown that spike stall is due to the stall occurring at the tip. 3-Dimensional effects arising from radial flow variation is necessary to capture spike stall. In Moore-Greitzer model, radial variation is not considered. Hence, tip stall cannot be captured in Moore-Greitzer model; effectively every quantity is only evaluated at the mean. This necessitates some modification of the 2-D Moore-Greitzer model in order to overcome its deficiencies.

In the present paper, we will distinguish between modal and non-modal disturbances. Spiky disturbances, for example, will be included in non-modal disturbances. Single-mode and multimode disturbances within Moore-Greitzer model will be reviewed, and subsequently, the model will be augmented through the introduction of an additional variable r. Moore-Greitzer model subjected to single mode disturbance will be called single-mode Moore-Greitzer model while the model subjected to multimode disturbance will be called multimode Moore-Greitzer model. In particular, we compute multimodal solutions to the augmented Moore-Greitzer model and seek to construct a link between the 'new' multimodal solutions and rotating stall onset.

II. Single Mode Equation and Analysis

A detailed bifurcation analysis of the single mode Moore-Greitzer model was first presented by McCaughan.[5] She was able to predict the mechanisms for the onset of rotating stall and surge in terms of bifurcations of the axisymmetric equilibrium state. Agarwal and Ananthkrishnan[6] improved on this analysis, mainly in the context of surge onset and cessation.

The analysis of the Moore-Greitzer model can be greatly simplified by assuming that most of the energy of the rotating stall disturbance is concentrated in its first harmonic. With the help of this assumption and the Galerkin method, one obtains the following three differential equations for non-dimensionalized pressure rise (Ψ), non-dimensionalized flow coefficient (Φ), and the square of the amplitude of the fundamental harmonic (J) of the rotating stall disturbance:[5]

$$\dot{\Psi} = (1/\beta^2)(\Phi - \sqrt{(}\gamma\Psi) + 1) \quad (1)$$

$$\dot{\Phi} = -\Psi + \Psi_c - 3\Phi J \quad (2)$$

$$\dot{J} = \sigma J(1 - \Psi^2 - J) \quad (3)$$

where Ψ_c is taken as the cubic axisymmetric function:

$$\Psi_c = \Psi_{c0} + 1 + 1.5\Phi - 0.5\Phi^3 \quad (4)$$

The presence of circumferential perturbation ($J \neq 0$) in equilibrium solution indicates rotating stall in the Moore-Greitzer model. In steady state, from Eq. (3), there can be two solutions corresponding to $J = 0$ and $J = 1 - \Phi^2$. First solution corresponds to steady axisymmetric solution: $\Psi = \Psi_c$ and $\Phi = \sqrt{(}\gamma\Psi) + 1$. The other solution pertains to rotating stall with $\Psi = \Psi_c - 3\Phi(1 - \Phi^2)$. Steady state solutions with their stabilities are found through bifurcation analysis using AUTO software.[8] Figure 2 is the bifurcation diagram of non-dimensionalized pressure rise against non-dimensionalized flow coefficient.

The solid lines in Fig. 2 represent stable solutions while the dotted lines represent unstable solutions. The peak of the axisymmetric curve can be identified at $\Phi = 1$ and $\Psi = \Psi_{peak}$. (Solutions with $\Psi > \Psi_{peak}$ are not physical because for those solutions J is negative, which is not possible as J is the square of the amplitude.) The peak point in Fig. 2 corresponds to a transcritical bifurcation. When the mass flow is throttled past the peak, the compressor stalls and the operating point jumps from the axisymmetric solution A to the stable rotating stall solution B. This jump is seen clearly in Fig. 3 which is a bifurcation diagram of Ψ versus the throttle parameter, γ. The peak of the compressor characteristic can be identified by the transcritical bifurcation point at the peak. Now, when mass flow is marginally throttled, the solution jumps vertically down to the stable branch labeled B (as shown by arrow), which corresponds to rotating stall equilibrium. Now, if one were to increase to increase the throttle, the system will continue to lie on curve B till it jumps back to curve A as shown by arrow in Fig. 3. Thus, a hysteresis loop is formed. So, Moore-Greitzer model subjected to single mode disturbance predicts that the compressor will stall at the peak of the compressor characteristic curve.

III. Multimode Equations

In general the Moore-Greitzer equations for the multimode disturbances are of following form:[7]

$$\frac{d\Psi}{d\xi} = \frac{1}{4B^2 l_c}\left[\Phi - \Phi_T\right] \quad (5)$$

$$\frac{d\Phi}{d\xi} = \frac{1}{l_c}\left[-\Psi(\xi) + \frac{1}{2\pi}\int_0^{2\pi} \Psi_c\left(\Phi + \left(\tilde{\phi}'_\eta\right)_0\right)\, d\theta\right] \quad (6)$$

$$\dot{A}_k = \frac{1}{\pi}\frac{k}{m + k\mu}\left[\int_0^{2\pi} \Psi_c\left(\Phi + \left(\tilde{\phi}'_\eta\right)_0\right)\cos(k\theta - \Theta_k)\, d\theta\right] \quad (7)$$

$$\dot{\Theta}_k = \frac{k}{m + k\mu}\left[\frac{-k\mu}{2} + \frac{1}{\pi A_k}\int_0^{2\pi} \Psi_c\left(\Phi + \left(\tilde{\phi}'_\eta\right)_0\right)\sin(k\theta - \Theta_k)\, d\theta\right] \quad (8)$$

where A_k and Θ_k correspond to the amplitude and phase of the k^{th} mode. Humbert and Krener[7] analyzed the above equations for phase locked solutions, though there are some disadvantages associated with these

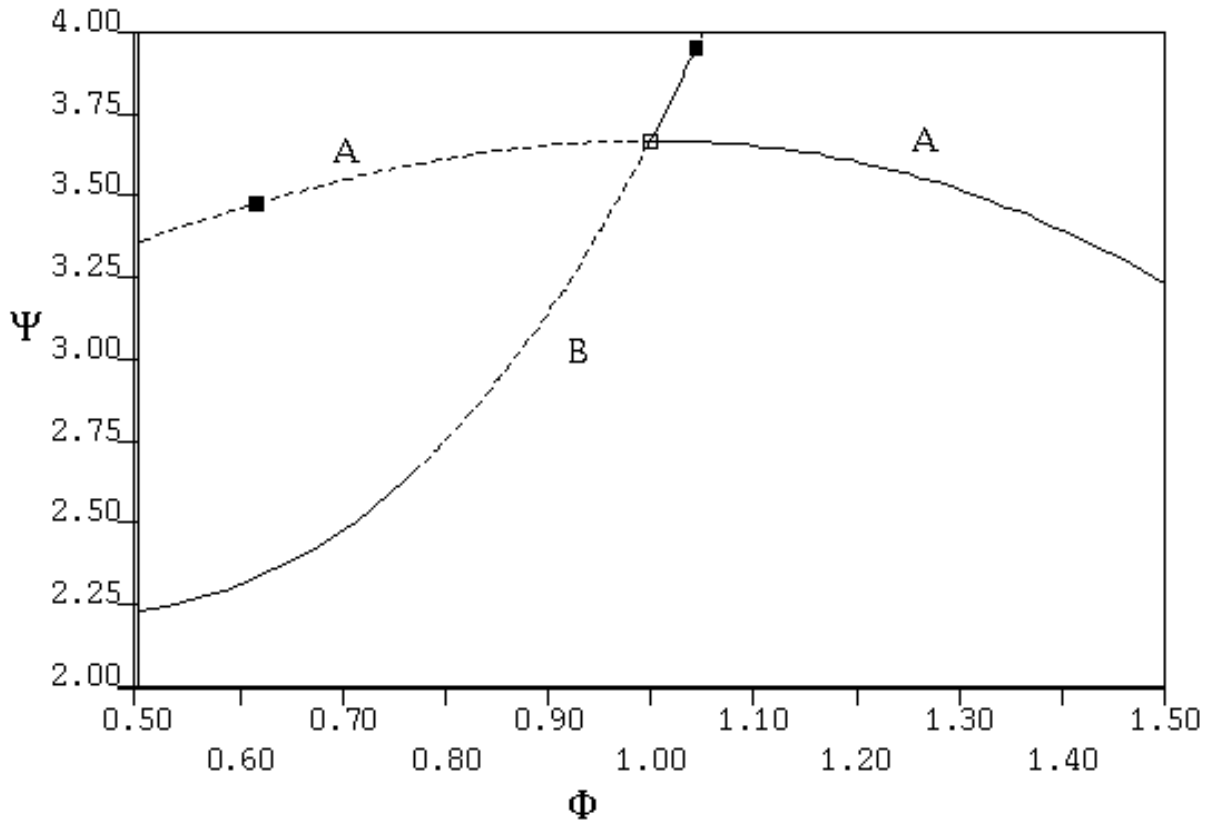

Figure 2. Ψ **vs** Φ **for single-mode Moore-Greitzer model (A: axisymmetric solution (**$J = 0$**); B: equilibrium solutions with** $J \neq 0$**) (solid line: stable solutions; dotted line: unstable solutions)**

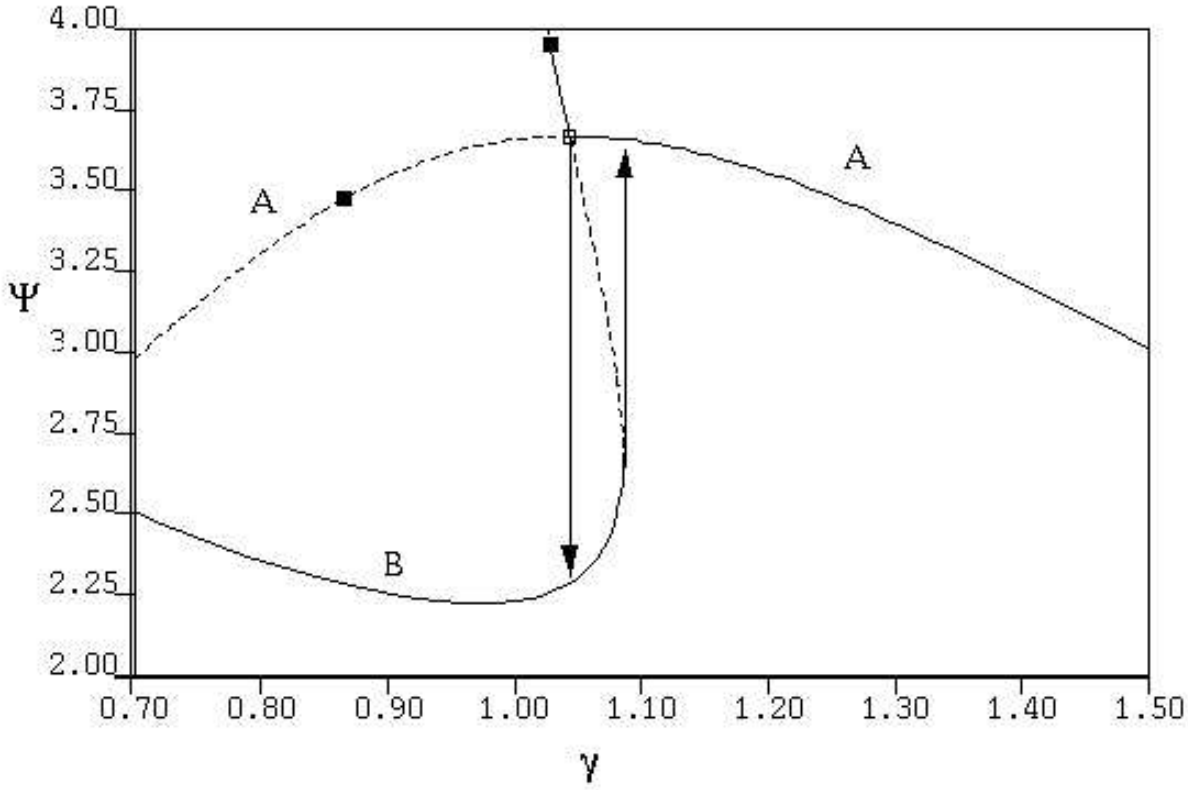

Figure 3. Ψ **vs** γ **for single-mode Moore-Greitzer model (A: axisymmetric solution (**$J = 0$**); B: equilibrium solutions with** $J \neq 0$**) (solid line: stable solutions; dotted line: unstable solutions)**

equations. The problem is in Eq. (8) for the phase variables due to terms containing A_k's in the denominator. The phase equations are then singular for the axisymmetric case where all the A_k's are identically zero. More significantly, they are actually not valid at all those instants of time where any of A_k's are zero. Thus during a numerical simulation, if any of the A_k's become zero, which can occur in transients, the equations become invalid. To overcome this problem, Humbert and Krener[7] ignored the axisymmetric case and analyzed only non-axisymmetric flow conditions.

The other question pertains to the angle at which these phases get locked. The angle is chosen such that higher harmonics too have their nodes at the fundamental harmonic's nodes. So, the phase locking angles (α_k) are taken as 0 and π. The solutions are found for relative phase angle equal to 0 and π and the two solutions are appended to get the full picture. As, the phase locking angles has been decided beforehand, phase equations (Eq. (8)) are no longer required and are discarded. The final equations are shown below and the singularity has been eliminated as the phase equations have been removed.

$$\frac{d\Psi}{d\xi} = \frac{1}{4B^2}\left[\Phi - \Phi_T\right]\frac{1}{l_c} \tag{9}$$

$$\frac{d\Phi}{d\xi} = \frac{1}{l_c}\left[-\Psi(\xi) + \frac{1}{2\pi}\int_0^{2\pi} \Psi_c\left(\Phi + \left(\tilde{\phi}'_\eta\right)_0\right)\, d\theta\right] \tag{10}$$

$$\dot{A}_k = \frac{1}{\pi}\frac{k}{m+k\mu}\left[\int_0^{2\pi} \Psi_c\left(\Phi + \left(\tilde{\phi}'_\eta\right)_0\right)\cos(k\theta - \Theta_k)\, d\theta\right] \tag{11}$$

A. Two-Mode Model Analysis

The equations for the two-mode Moore-Greitzer model is given below using the numerical data from:[7]

$$\dot{\Psi} = (1/\beta^2)(\Phi - \gamma\sqrt{(}\Psi) + 1) \tag{12}$$

$$\dot{\Phi} = -\Psi + \Psi_c - 0.75\Phi(A_1^2 + A_2^2) - 0.375A_1^2A_2 cos(\alpha_1) \tag{13}$$

$$\dot{A}_1 = 0.72(0.5A_1 - 0.125A_1^3 - 0.25A_1A_2^2 - 0.5A_1\Phi^2 - 0.5A_1A_2\Phi cos(\alpha_1)) \tag{14}$$

$$\dot{A}_2 = 0.72(0.75A_2 - 0.375A_1^2A_2 - 0.1875A_2^3 - 0.75A_2\Phi^2 - 0.375A_1^2\Phi cos(\alpha_1)) \tag{15}$$

where $\alpha_1 = 2\Theta_1 - \Theta_2$. In the present analysis, Ψ_c is taken as the cubic axisymmetric solution in Eq. (4). β is kept fixed at 0.5, while γ (throttle parameter) is the continuation parameter. The bifurcation diagram of non-dimensionalized pressure rise (Ψ) versus non-dimensionalized flow coefficient (Φ) is shown in Fig. 4.

There are three distinct curves seen in the bifurcation diagram (Fig. 4). The curve labeled A corresponds to $A_1 = 0$ and $A_2 = 0$, which is the cubic axisymmetric solution $\Psi = \Psi_c$. The curve labeled B corresponds to the single mode solution, $A_1 = 0, A_2 \neq 0$. This curve originates at the peak of curve A. The curve labeled C corresponds to the multimode solutions with $A_1 \neq 0$ and $A_2 \neq 0$. Corresponding curves on the plot of Ψ versus γ (Fig. 5), A_1 versus γ (Fig. 6) and A_2 versus γ (Fig. 7) are similarly labeled and can be identified.

In order to understand the bifurcation plots, we start from a high value of flow coefficient (Φ). Then, the system will lie on stable part of the axisymmetric curve A to the right of the peak. Now, Φ is continuously decreased by reducing the throttle and the solution moves along the axisymmetric curve until it encounters a bifurcation point at the peak pressure rise point and the compressor dynamics enters rotating stall. In the stalled condition, the pressure rise drops drastically and the system plunges vertically from curve A to curve C in Fig. 5 as shown by the arrow. The corresponding jumps in A_1 and A_2 can be found from Figs. 6 and 7 respectively. Now, if one were to increase the throttle, the system will continue to lie on curve C till it encounters a saddle-node bifurcation and the system will jump back to the axisymmetric curve A at a point to the right of the peak as shown by the arrow. Thus, a hysteresis loop is formed.

Now, we can compare the one-mode and two-mode solutions. Two-mode equations clearly bring out the coupling between the two modes. The equation for A_2 in particular has a term which is independent of A_2 but is a function of A_1. This shows that the lower modes (in this case A_1) can trigger the higher modes (in this case A_2) even if the higher mode was initially dormant. Also, Figs. 3 and 5 show larger region of hysteresis for the two-mode case when compared to single-mode case. The two-mode solution curve (curve C in Fig. 5) is tangent at the peak to the curve A, while for the one-mode case, the intersection of axisymmetric and rotating stall curves in Fig. 3 is transverse. Above results in decrease in region of attraction of axisymmetric equilibrium points near the peak of the compressor characteristic for the two-mode case compared to one-mode solutions. In spite of the differences between the two cases, the stall point is still at the peak of the compressor characteristics.

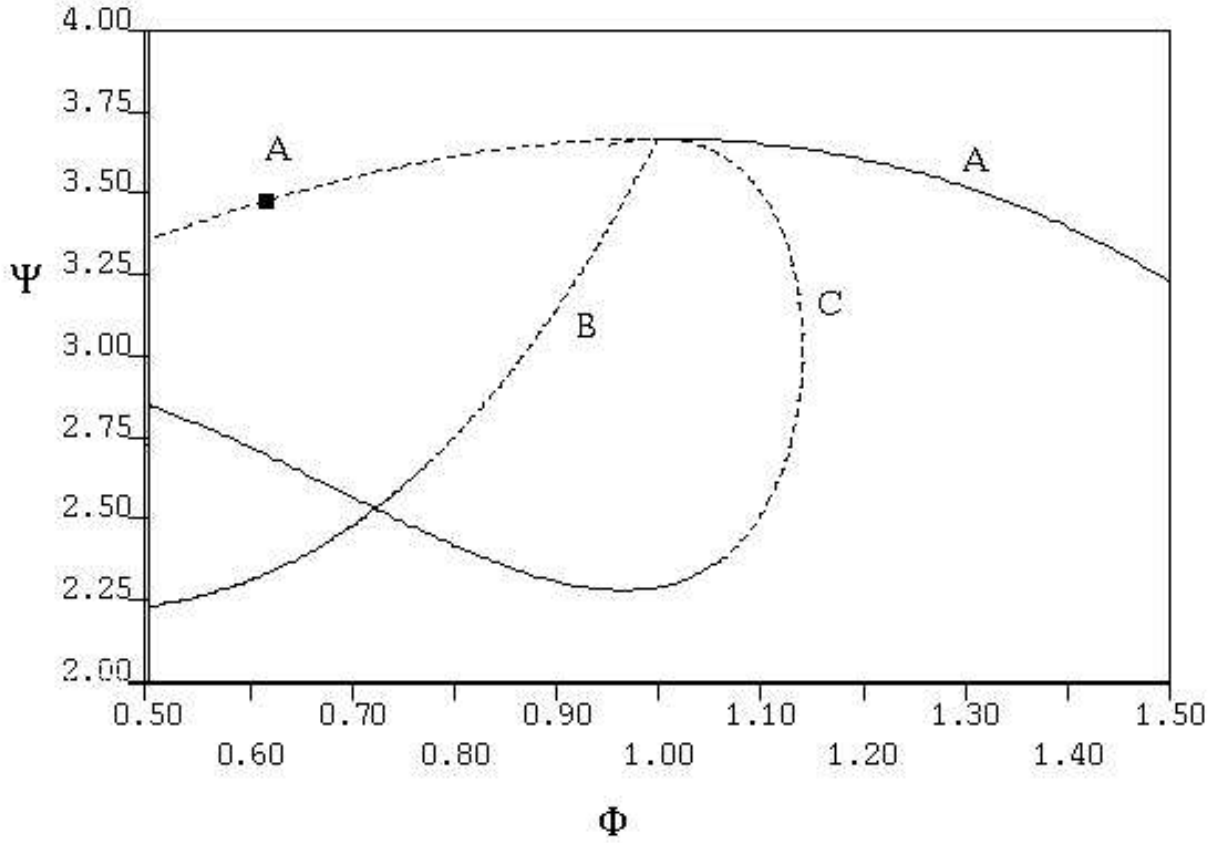

Figure 4. Ψ vs Φ for two-mode Moore-Greitzer model (A: axisymmetric solution ($A_1 = 0, A_2 = 0$); B: equilibrium solutions with $A_1 = 0, A_2 \neq 0$; C: equilibrium solutions with $A_1 = 0, A_2 = 0$) (solid line: stable solutions; dotted line: unstable solutions)

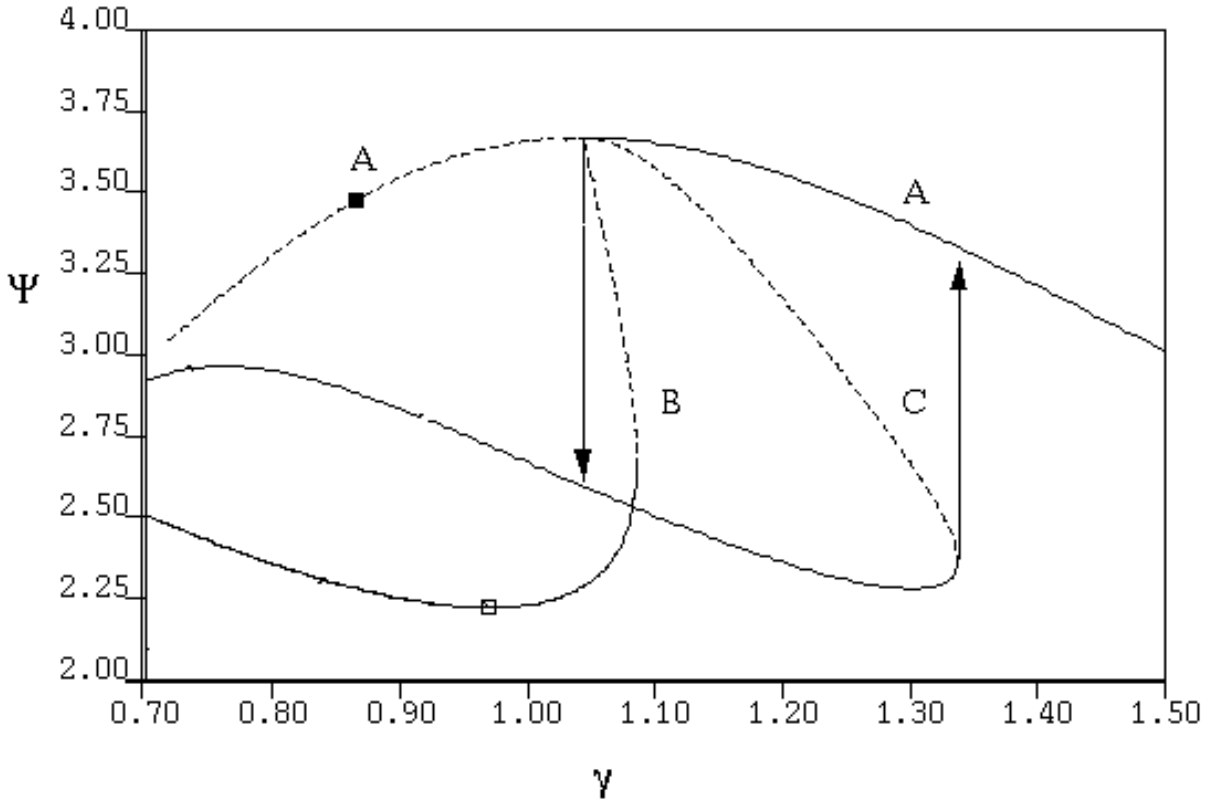

Figure 5. Ψ vs γ for two-mode Moore-Greitzer model (A: axisymmetric solution ($A_1 = 0, A_2 = 0$); B: equilibrium solutions with $A_1 = 0, A_2 \neq 0$; C: equilibrium solutions with $A_1 = 0, A_2 = 0$) (solid line: stable solutions; dotted line: unstable solutions)

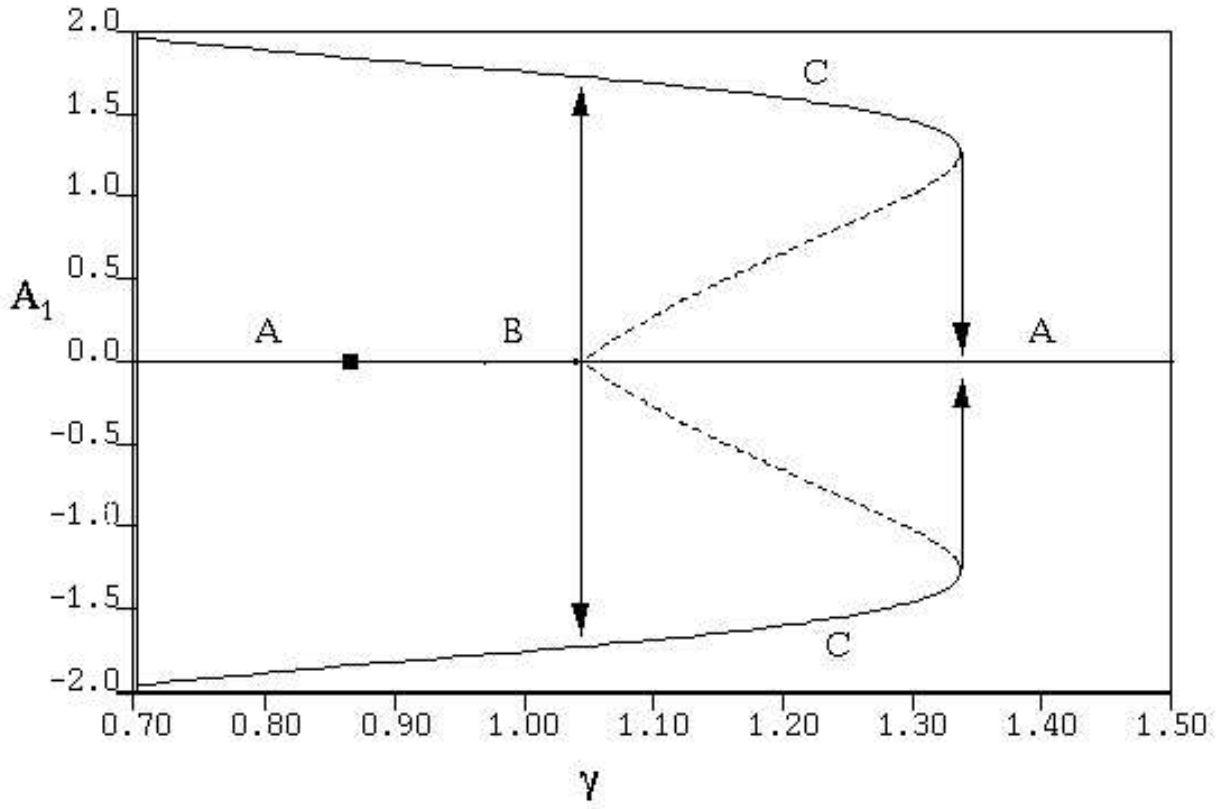

Figure 6. A_1 **vs** γ **for two-mode Moore-Greitzer model (A: axisymmetric solution (**$A_1 = 0, A_2 = 0$**); B: equilibrium solutions with** $A_1 = 0, A_2 \neq 0$**; C: equilibrium solutions with** $A_1 = 0, A_2 = 0$**) (solid line: stable solutions; dotted line: unstable solutions)**

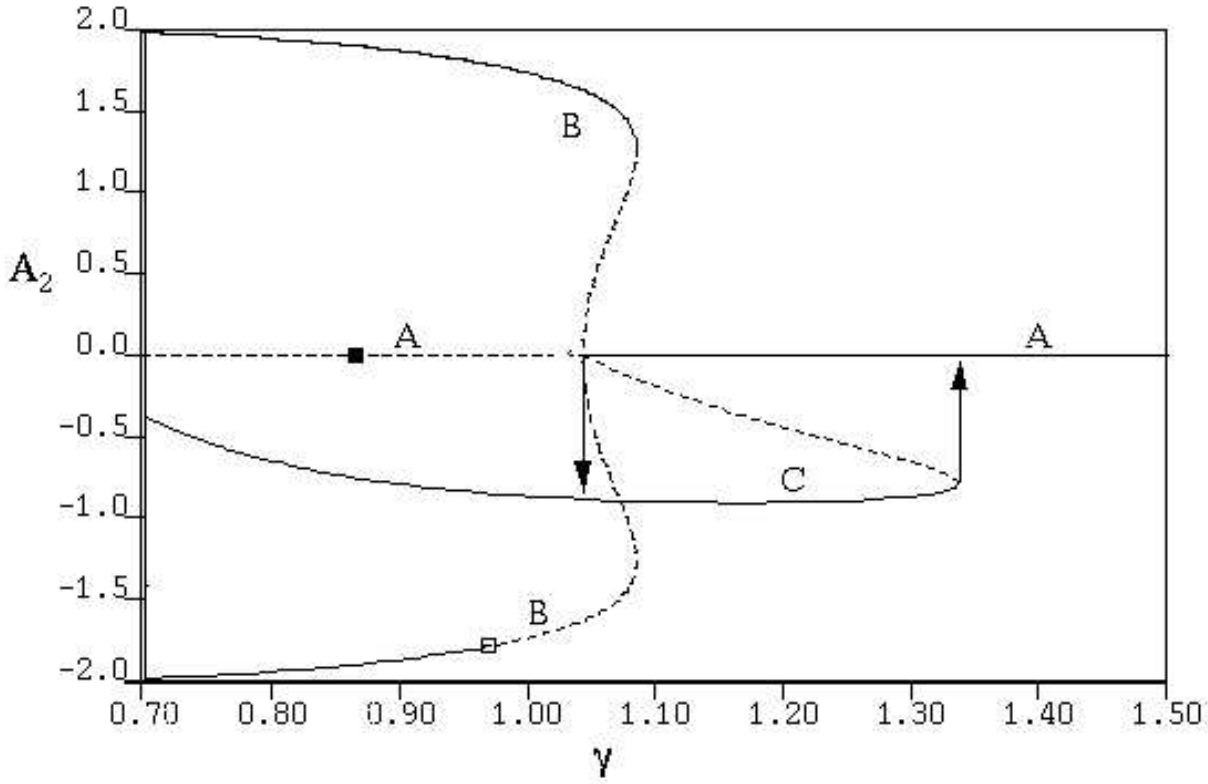

Figure 7. A_2 **vs** γ **for two-mode Moore-Greitzer model (A: axisymmetric solution (**$A_1 = 0, A_2 = 0$**); B: equilibrium solutions with** $A_1 = 0, A_2 \neq 0$**; C: equilibrium solutions with** $A_1 = 0, A_2 = 0$**) (solid line: stable solutions; dotted line: unstable solutions)**

The bifurcation analysis was also done for three-mode Moore-Greitzer model and it was found to be qualitatively similar to the two-mode case. Thus, two-mode Moore-Greitzer model can be said to be representative of the multimode Moore-Greitzer model. Next, it is necessary to modify the model in order to correctly predict the stall point when the compressor is subjected to disturbances which are different from the modal form. The modifications are discussed in the next section.

IV. Modifications to the Moore-Greitzer Model

From the previous sections, it is clear that Moore-Greitzer model predicts the peak as the point of the onset of instability for both single-mode and multimode case. But, from past experience, it is known that compressors do stall to the right of the peak as well. So, some modification is required in the model to incorporate non-modal stall onset to the right of the peak of the compressor characteristic. Firstly, we evaluate some of the assumptions made in the model. It was assumed that that there is no radial velocity, $C_r = 0$. Also, as the axial velocity is uniform, $\frac{dC_a}{dr} = 0$. Also, as the onset of rotating stall is same at every radial station, flow incidence angles are constant along the span. In the present analysis, it is assumed that actuator disk model of Moore-Greitzer model can be replaced by blades with identical blade sections from root to tip. Hence, blade sections will be same from root to tip and specific work done is constant along the span.

A. Variable r

In order to modify the Moore-Greitzer model, we assume non-uniform axial velocity (C_a) along the span accompanied by radial flow to satisfy continuity equation. Now, flow incidence angles will vary from root to tip resulting in different loading at various radial sections which had uniform loading previously. Now, suppose that the blade loading changes such that tip loading is greater than the hub loading, possibly due to greater flow incidence angle at the tip than at the hub. In the present case, the reference mean may not be geometric mean of the compressor. Reference mean might shift towards the tip as the tip region is more loaded than the hub region. So, Reference mean would have higher blade speed than the geometric mean. This would suggest compressor characteristic corresponding to increased blade RPM.

In order to implement above changes in the Moore-Greitzer model, a variable r is defined as a measure of the change in flow incidence angle (hence, loading) at the reference mean of the blade. r is defined as the difference between the slope of the tangent of the flow incidence angle of the new loading and the previous constant loading. As the slope of flow incidence angle of original Moore-Greitzer model is zero, r is simply the slope of the tangent of the flow incidence angle (i) at the reference mean of the augmented Moore-Greitzer model.

$$r = \frac{d\tan i}{dR}\Big|_{R_P} \tag{16}$$

where, R_P is reference mean of the compressor.
In order to derive the expression for r in terms of blade geometry angles, the equation for $\tan i$ is written from the velocity triangles at rotor inlet at blade reference mean (same as geometric mean) for the first case (original Moore-Greitzer model).

$$\tan i = \frac{(\frac{R/R_m}{\Phi} - \frac{C_{w1}/U_m}{\Phi}) - \tan\beta_1'}{1 + (\frac{R/R_m}{\Phi} - \frac{C_{w1}/U_m}{\Phi})\tan\beta_1'} \tag{17}$$

where, R_m is mean radius, C_{w1} is circumferential velocity at rotor inlet, and β_1' is blade inlet angle.
Above equation is differentiated with respect to Radius (R) and $\frac{d\tan i}{dR} = 0$ is used to arrive at an expression in terms of other quantities. Similarly, equation of $\tan i$ for the augmented Moore-Greitzer model is written and differentiated. In the second case, R_m, U_m, C_{w1} and Φ would be different as the reference mean might shift toward the tip. But, as the blade geometry remains the same, β_1' will remain the same. The expression derived from first case is used to eliminate $\frac{d\tan\beta_1'}{dR}$. The resultant expression is applied at the reference mean of the augmented Moore-Greitzer model. Finally, the expression of r is obtained as shown below:

$$r = \frac{a{\Phi_p}^2 + b\Phi_p + c}{(\Phi_p + d)^2} \tag{18}$$

where, Φ_p is non-dimensionalized flow coefficient at the reference mean of augmented Moore-Greitzer model, and a, b, c, d are constants.
The expressions for the four constants a, b, c, d are given below:

$$a = -\left((1+\tan^2\beta_1') \frac{\left(\frac{\Phi_m}{R_m} - \frac{\Phi_m}{U_m}\frac{dC_{w1}}{dR}\right)}{\left(\Phi_m^2 + (\frac{R}{R_m} - \frac{C_{w1}}{U_m})^2\right)} \right) \Bigg|_{R_m} \tag{19}$$

$$b = \left((1+\tan^2\beta_1') \Big(\frac{1}{R_m} - \frac{1}{U_m}\frac{dC_{w1}}{dR} \Big) \right) \Bigg|_{R_P} \tag{20}$$

$$c = -a \left(\Big(\frac{R}{R_m} - \frac{C_{w1R}}{U_m} \Big)^2 - (1+\tan^2\beta_1') \Big(\frac{R}{R_m} - \frac{C_{w1R}}{U_m} \Big) \frac{d\Phi_R}{dR} \right) \Bigg|_{R_P} \tag{21}$$

$$d = \left(\Big(\frac{R}{R_m} - \frac{C_{w1R}}{U_m} \Big) \tan\beta_1' \right) \Bigg|_{R_P} \tag{22}$$

Now, r in Eq. (18) is used as a variable to form the fifth equation of the two-mode Moore-Greitzer model. Also, $r\Phi_p$ is added to the Eq. (14) to obtain the following equations:

$$\dot{\Psi} = (1/\beta^2)(\Phi_p - \gamma\sqrt{(}\Psi) + 1) \tag{23}$$

$$\dot{\Phi_p} = -\Psi + \Psi_c - 0.75\Phi_p(A_1^2 + A_2^2) - 0.375A_1^2A_2 cos(\alpha_1) + \mathbf{r(\Phi_p)} \tag{24}$$

$$\dot{A_1} = 0.72(0.5A_1 - 0.125A_1^3 - 0.25A_1A_2^2 - 0.5A_1{\Phi_p}^2 - 0.5A_1A_2\Phi_p cos(\alpha_1)) + \mathbf{(0.72)(0.5)qA_1} \tag{25}$$

$$\dot{A_2} = 0.72(0.75A_2 - 0.375A_1^2A_2 - 0.1875A_2^3 - 0.75A_2{\Phi_p}^2 - 0.375A_1^2\Phi_p cos(\alpha_1)) + \mathbf{(0.72)(0.75)qA_2} \tag{26}$$

$$\dot{\mathbf{r}} = \mathbf{r}\Big(\mathbf{r} - \frac{\mathbf{a{\Phi_p}^2 + b\Phi_p + c}}{\mathbf{(\Phi_p + d)^2}} \Big) \tag{27}$$

Equations (24)-(27) defines the system for augmented two-mode Moore-Greitzer model. Terms added to the Moore-Greitzer model are shown in bold. Equations (26) and (27), both, have an additional term containing a parameter q which will be discussed later. Equation (27) has two steady state solutions: $r = 0$ corresponds to the original Moore-Greitzer solution. Second solution corresponds to Eq. (18).

Figure 8 is the bifurcation diagram of non-dimenzionalised pressure rise (Ψ) versus non-dimenzionalised flow coefficient at reference mean (Φ_P). In Fig. 8, non-zero A_1 and A_2 solutions are not shown for clarity. Solid lines represent stable steady state solutions while dotted lines correspond to unstable solutions. The point of onset of instability is shown in Fig. 8 by empty square which corresponds to transcritical bifurcation. The diagram is capable of showing non-modal rotating stall to the right of peak of the original compressor characteristic. In this case, onset of rotating stall is non-modal because modal stall occurs at the peak of the compressor characteristic curve. The original compressor characteristic curve has $r = 0$. The effect of non-zero r is to form another, modified, characteristic curve, whose peak is to the right of the peak of the original curve (higher Φ). This can be explained in the following manner. As r increases, flow incidence angle increases resulting in higher loading on the blade which gives more pressure rise (Ψ). Also, due to more loading, the compressor will stall at higher flow coefficient (Φ), explaining the position of modified characteristic peak higher and to the right of the peak of the original curve. Camp and Day[4] have shown the variation of the first stage compressor characteristic with different inlet guide vane stagger angles obtained from experiments. As stagger was decreased, the compressor stalled to right of the peak of the compressor characteristic, which is exactly the same as the shift of the peak of the modified curve in the augmented Moore-Greitzer bifurcation diagram in Fig. 8.

Thus, by introducing variable r and parameter q to the Moore-Greitzer model, it is possible to predict rotating stall to the right of the peak. The point of onset of rotating stall is the intersection of the two curves. Value of parameter q is set such that it accounts for the shift in hysteresis associated with the shift of the point of onset of rotating stall which was at the peak for the original Moore-Greitzer model. Figure 9 is the diagram of Ψ versus Φ_P with $q = 0$. Figure 9 show that the curves C and N emerge from curve A and M respectively at $\Phi_P = 1$ which correspond to peak for the original Moore-Greitzer model. Curves C and

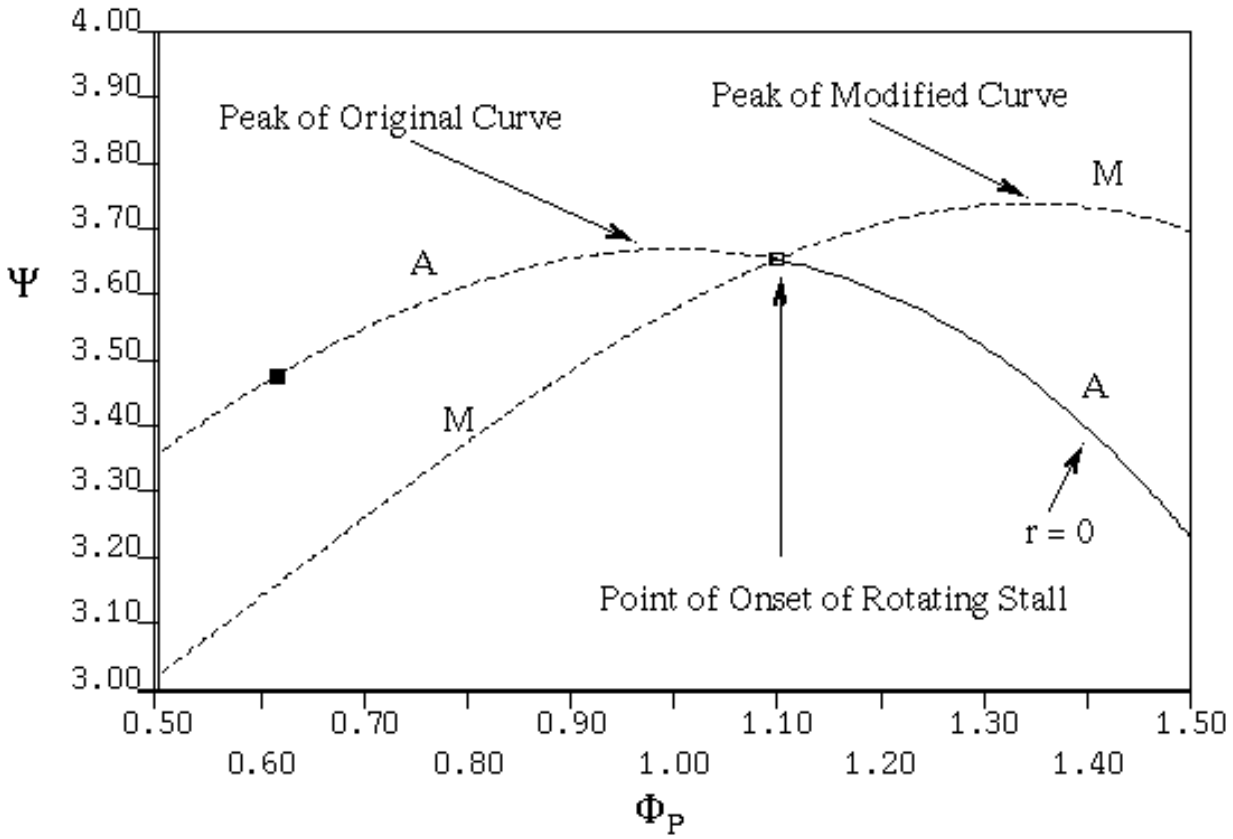

Figure 8. Plot of Ψ vs Φ_p for augmented two-mode Moore-Greitzer model (A: axisymmetric solutions ($r = 0, A_1 = 0, A_2 = 0$); M: equilibrium solutions with $r \neq 0, A_1 = 0, A_2 = 0$; unfilled square: point of onset of rotating stall) (solid lines: stable solutions; dotted lines: unstable solutions)

N correspond to nonzero A_1 and A_2 solutions for $r = 0$ and $r \neq 0$ respectively. Now, the effect of q can be seen in Fig. 10 where the curves C and N shift to the right of the peak (as shown by arrow) to emerge from curve A and M respectively at exactly the intersection point of the two curves. This point of intersection is also the point of onset of instability. So, the effect of q is to ensure that all the four curves have a common intersection point. The study of any other q on the system will be undertaken in future studies.

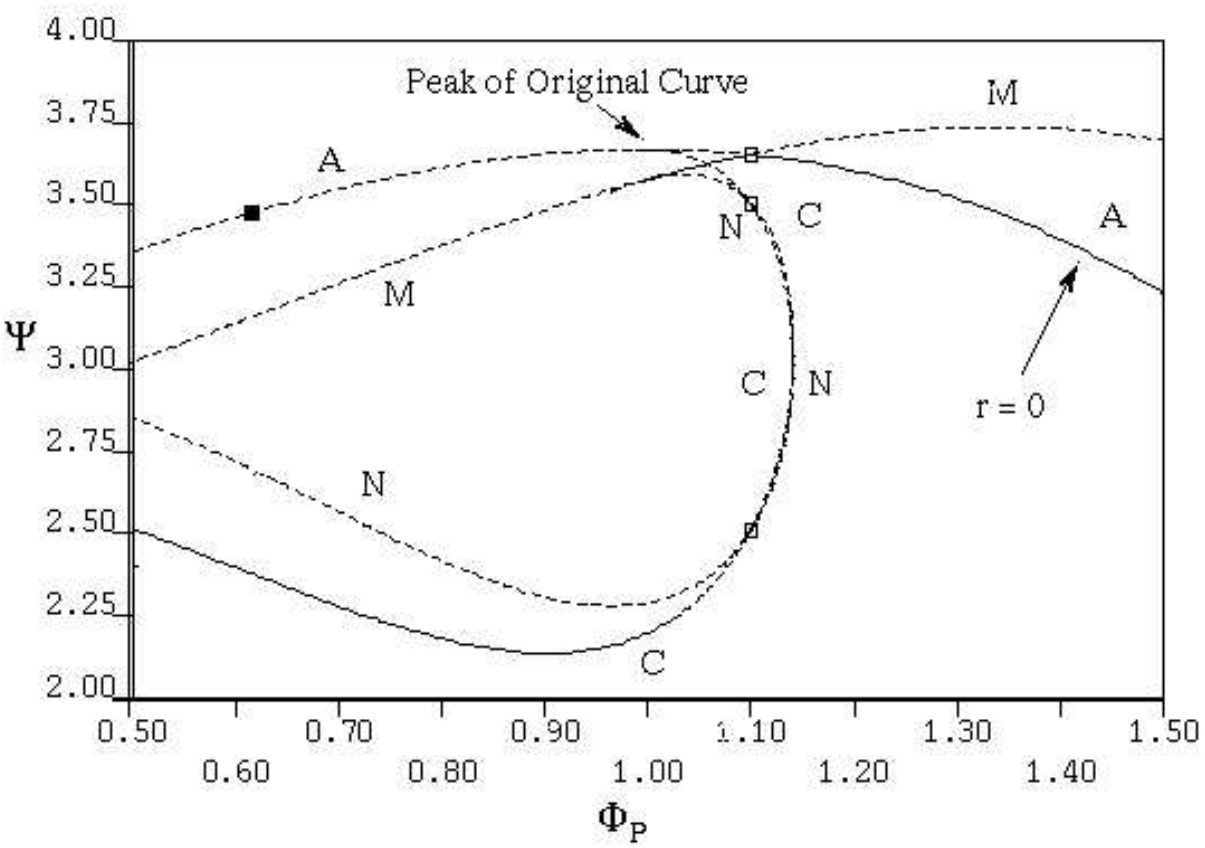

Figure 9. Plot of Ψ vs Φ_p for augmented two-mode Moore-Greitzer model with $q = 0$ (A: axisymmetric solution ($r = 0, A_1 = 0, A_2 = 0$); M: equilibrium solutions with $r \neq 0, A_1 = 0, A_2 = 0$; C: equilibrium solutions with $r = 0, A_1 \neq 0, A_2 \neq 0$; N: equilibrium solutions with $r \neq= 0, A_1 \neq 0, A_2 \neq 0$; unfilled square: point of onset of rotating stall) (solid lines: stable solutions; dotted lines: unstable solutions)

It is possible that for some compressors, the two curves do not intersect at all. This is determined by the value of the four constants (a, b, c and d) for that compressor. In that case, compressor will stall at the peak of the compressor characteristic curve and this stall will be modal. The exact location of the instability point will depend on the four constants, a, b, c and d. These constants will depend on the blade geometry and the methodology by which the compressor is designed. The methodology includes the design radial variation of circumferential and axial velocity. Once, the four constants are known for a given compressor, the instability point can be found from the bifurcation diagram.

V. Conclusion

It is known that the Moore-Greitzer model predicts modal stall at and after the flow is throttled past the peak point on the compressor characteristic curve. It also predicts that the compressor will be stable to modal disturbances to the right of the peak. Moore-Greitzer model is extended by adding an additional equation in variable r and introducing parameter q to account for shift in hysteresis associated with shift in point of onset of rotating stall. r depends on the flow incidence angle at the reference mean of the

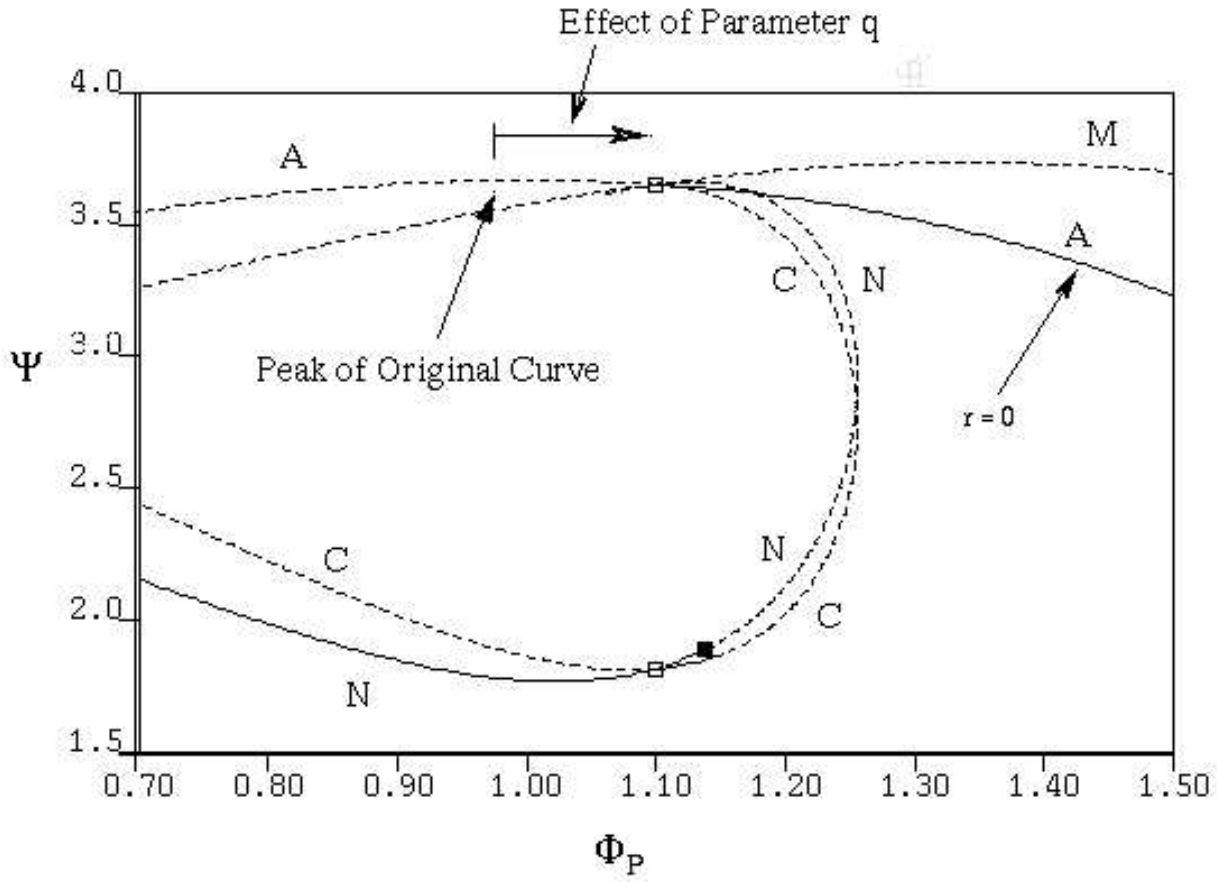

Figure 10. Plot of Ψ vs Φ_p for augmented two-mode Moore-Greitzer model with $q \neq 0$ (A: axisymmetric solution ($r = 0, A_1 = 0, A_2 = 0$); M: Equilibrium solutions with $r \neq 0, A_1 = 0, A_2 = 0$; C: equilibrium solutions with $r = 0, A_1 \neq 0, A_2 \neq 0$; N: equilibrium solutions with $r \neq 0, A_1 \neq 0, A_2 \neq 0$; unfilled square: point of onset of rotating stall) (solid lines: stable solutions; dotted lines: unstable solutions)

compressor. Above modifications result in creating another curve on the bifurcation diagram which cuts the original curve to the right of the peak of the compressor characteristic. The intersection point between the two curves gives the point of onset of rotating stall in the compressor. Also, for some compressors, the two curves will not cross and these compressors will undergo modal stall at the peak. Thus, using the augmented Moore-Greitzer model, it is possible to predict the stall onset point to the right of the peak of the compressor characteristic curve. This study is expected to help in explaining the phenomenon of rotating stall inception observed to the right of the peak in the compressor characteristic.

A through analysis of the four constants a, b, c, d will be done in future studies. Also, the effect of parameter q and its physical significance will be extensively studied in future.

Acknowledgements

The authors would like to acknowledge the support of Pratt and Whitney, Canada who funded this research. Also, we would like to thank Dr. Gavin Hendricks of Pratt and Whitney for his invaluable suggestions.

References

[1]Willems, F., and de Jager, B., " Modeling and Control of Compressor Flow Instabilities," *IEEE Control Systems Magazine*, Vol. 19, No. 5, 1999, pp. 8-18.

[2]Moore, F., and Greitzer, E.M.,"A Theory of Post-Stall Transients in Axial Compressors: Part I- Development of the Equations," *ASME Journal of Engineering for Gas Turbines and Power*, Vol. 108, No. 1, 1986, pp. 68-76.

[3]Day, I.J., "Stall Inception in Axial Flow Compressors," *Journal of Turbomachinery*, Vol. 115, No. 1, 1993, pp. 1-9.

[4]Camp, T.R., and Day, I.J., "A Study of Spike and Modal Stall Phenomena in a Low-Speed Axial Compressor," *Journal of Turbomachinery*, Vol. 120, No. 6, 1998, pp. 393-401.

[5]McCaughan, F.E., "Application of Bifurcation Theory to Axial Flow Compressor Instability," *ASME Journal of Turbomachinery*, Vol. 111, No. 10, 1989, pp. 426-433.

[6]Agarwal, A., and Ananthkrishnan, N., "Bifurcation Analysis for Onset and Cessation of Surge in Axial Flow Compressors," *International Journal of Turbo and Jet Engines*, Vol. 17, No. 2, 2000, pp. 207-217.

[7]Humbert, J.S. and Krener, A.J., "Dynamics and Control of Entrained Solutions in Multi-Mode Moore-Greitzer Compressor Models," *International Journal of Control*, Vol. 71, No. 5, 1998, pp. 807-821.

[8]Doedel, E.J., Champneys, A.R., Fairgrieve, T.F., Kuznetsov, Y.A., Sandstede, B., and Xang, X., "AUTO 97: Continuation and Bifurcation Software for Ordinary Differential Equations," Department of Computer Science, Concordia University, 1997.